33rd Annual International Conference of the IEEE EMBS
Boston, Massachusetts USA, August 30 - September 3, 2011

Slowed Propagation Across the Compacta-Trabeculata Interface: A Consequence of Fiber and Sheet Anisotropy.

Stephen H. Gilbert, Alan P. Benson, Richard D. Walton, and Olivier Bernus.

Abstract— **Transmural myocardial activation is influenced by myocardial structure, including structural differences between the compacta (Cta) and the trabeculata (Tta), although this has not been fully explained. Hearts from rats were Langendorff perfused, stained with DI-4-ANEPPS, the apex was cut off and fluorescence acquired from the exposed short-axis surface. The hearts were stimulated at 160 ms cycle length at the anterior, lateral, posterior left ventricle (LV) and septal sub-epicardial sites. Conduction velocity perpendicular to the wave front orientation was measured in each pixel using a gradient-based approach. After optical mapping the cut surface was imaged using a light microscope and the extent of the Cta and Tta mapped and validated against 50µm isotropic MRI images. We used a 3D rat ventricle computational model, with architecture obtained from 200 µm isotropic diffusion tensor MRI and kinetics from the modified Pandit model to determine the relative roles of fibers and sheets on propagation. We show in the experimental study that circumferential propagation around the LV cavity is fast in the Cta: 63.2±19.5 and is slower in the Tta: 32.7±11.0* (mean ± s.d cm·s-1, * $p < 0.01$ by two sample t test). In the simulation study the pattern and velocity are not replicated in an isotropic model (I), are partially replicated in a simulation study including fiber anisotropy (A) and is more fully replicated in orthotropic (O) ventricles (fiber and sheet anisotropy), where the circumferential propagation velocity is, I: Cta: 54.2±3.9; Tta:54.3±3.9; A: Cta:43.6±3.2; Tta: 40.6±6.6; O: Cta: 63.2±19.5; Tta: 32.7±11.9*. We show that sheet orientation is important in understanding activation differences between Cta and Tta.**

I. Introduction

VENTRICULAR tachycardia (VT) and fibrillation (VF) are a major cause of morbidity and mortality in developed countries, however the detail of the initiation, propagation, progression and termination of these arrhythmias are not fully understood [1]. An important determinant of the propagation of arrhythmia is the structurally non-uniform myocardial substrate. It has recently been demonstrated that the myocardium is electrically orthotropic, with conduction in the ratio 4:2:1 along the myofibres, parallel to myolaminae and normal to myolaminae [2]. Furthermore, it has been hypothesized that structural complexity may be implicated in the transition from VT to VF when a single re-entrant wave (scroll wave) of excitation breaks down into multiple wavelets [3]. Thus, understanding the structural complexity of the myocardium and the impact of this structural complexity on the anisotropy/orthotropy of conduction will allow the understanding of the dynamics of re-entrant scroll waves.

Optical mapping of perfused hearts and perfused ventricular wedges enables high-resolution visualization of 2D (two-dimensional) ventricular surface activity, and hence concurrent activity on the endocardium, epicardium and on transmural cut surfaces, whilst 3D (three-dimensional) optical mapping of intramural activity is still at the proof of concept stage [4]. Computational simulations using verified models of cardiac geometry, architecture and excitation therefore allow the study of propagation inside the ventricular wall at sub-millimeter resolution [5] that cannot yet be achieved experimentally. A long recognized macroscopic anatomical feature of the myocardium is its division into a sub-epicardial compact region and a sub-endocardial loose trabecular zone [6], henceforth referred to as the compacta (Cta) and trabeculata (Tta). The boundary between the compacta and the trabeculata is known as the trabeculata-compacta-interface (TCI). Unlike fiber and sheet structural organization, the compacta and trabeculata can be recognized and measured in routine clinical cardiac imaging [7]. Furthermore, it has been proposed that activation is influenced by structural differences between the compacta (Cta) and the trabeculata (Tta). In a simulation study [8] it was shown that activation through the complex structure of the Tta produced fragmented epicardial activation, replicating experimental studies of [9]. The aim of this study is to investigate the hypothesis that transmural myocardial structural complexity influences activation wave propagation.

II. Methods

A. Optical Mapping Experiments

Male Wistar rats (n = 7) weighing 230 to 250 g were killed in accordance with the Animals (Scientific Procedures) Act 1986. Hearts were rapidly dissected, the aorta was cannulated, and the hearts were perfused in

Manuscript received March 23, 2011. This work was supported in part by grants from the Medical Research Council (G0701785, S. H. Gilbert; G0701776, A. P. Benson), Engineering and Physical Sciences Research Council (EP/F065574/1, R. D. Walton and O. Bernus), and the Royal Society (RG081248, O. Bernus).

All authors are with the Institute of Membrane and Systems Biology, Faculty of Biological Sciences, Multidisciplinary Cardiovascular Research Centre, University of Leeds, Leeds LS2 9JT, United Kingdom phone: +44-113-3431869; fax: +44-113-34342285; e-mail: s.h.gilbert@ leeds.ac.uk). Olivier Bernus is also with the Institut de Rhytmologie et Modelisation Cardiaque, Université Bordeaux Segalen, Centre Hospitalier Universitaire de Bordeaux, Hôpital Haut-Lévêque, Avenue de Magellan, 33604, Pessac Cedex, France.

Langendorff mode with a bicarbonate-buffered saline solution. Perfusion was maintained at a rate of 7 ml·min-1 for each experiment. The first group of hearts (n = 4) were first stained with DI-4-ANEPPS (2 ml as a 5 µg/ml bolus). Contraction was prevented with a 10 ml bolus of blebbistatin (0.06 µ mole/ml) [10]. After the complete cessation of contraction the apex was removed with a single equatorial short axis incision (5 ± 1 mm from the cardiac apex) using a microtome blade. The continued inhibition of contraction was ensured by supplementation of 15 µM blebbistatin to the perfusate. The heart was placed inside a plastic sleeve (12 mm diameter) with silver electrodes contacting the cut transmural myocardial surface near the epicardium at the anterior, lateral, posterior LV and RV or interventricular septum (IVS) (Fig 1). Excitation light from monochromatic LEDs, 530 nm (Cairn Research Ltd, Kent, UK), illuminated the cut transmural myocardial surface. Fluorescence was acquired using a broadband 700DF50 nm filter. Optical signals were acquired at 1,000 Hz and 0.4 mm spatial resolution using a CCD camera (SciMeasure Analytical systems, Decatur, GA) mounted with a Computar lens (focal length 8 mm, 1:1.2 aperture ratio; Computar, London, UK). Sub-epicardial stimulation was performed using a unipolar electrode (with a second electrode in superfusion bath) and a cycle length of 160 ms. Action potentials (APs) were acquired for 5 seconds at each pacing frequency and underwent ensemble averaging. Further temporal (1.5 ms kernel) and spatial (1.6 mm kernel) filtering was performed. Conduction velocity was calculated as in [11]. Radial conduction is defined as the conduction in the radial path from the stimulation point towards the centroid of the LV cavity, and circumferential conduction is defined as the conduction of the activation front parallel to this radius, around the ventricular cavity. In order to demonstrate homogenous dye loading and hence non-compromised perfusion, a second group of hearts (n = 3) were treated identically except that dye was loaded after transverse myocardial sectioning. Additionally it was demonstrated that APD, total ventricular activation times and normal sinus activation were consistent with reference values [12]. All hearts demonstrated a degree of electrotonic modulation of APD80, as shown in an example heart in Fig. 1. Total ventricular activation times of the LV took 26 ± 7 m/s.

B. *Myocardial structure*

After optical mapping the cut surface was imaged using a digital light microscope (Dino-Lite, AnMo, Taiwan) and the extent of the Cta and Tta mapped. The location of the TCI was confirmed by comparison to previously obtained high-resolution MRI images of rat hearts (FLASH MRI, 50 µm isotropic resolution [13]). Immediately after the completion of optical mapping one heart was perfusion fixed for 20 minutes at perfusion rate of 7 ml·min-1 with 4 % formaldehyde in bicarbonate-buffered saline, imaged using DT-MRI as in [12] in a 9.4 T MR instrument (Bruker BioSpin MRI GmbH, Ettlingen, Germany) at 200 µm isotropic resolution.

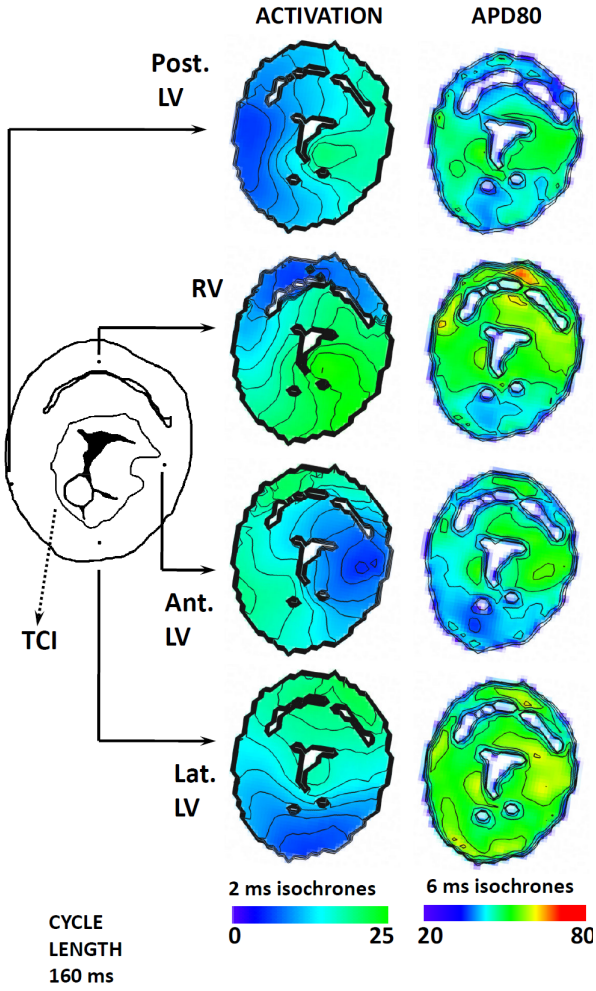

Fig. 1. Representative Activation maps (with 2 ms isochrones) and APD80 maps (with 6 ms isochrones) with the position of the unipolar stimulation electrodes shown. The TCI is labeled.

C. *Computer Simulations*

Simulations replicating the experimental protocol (pacing sites and cycle length) were carried out on heterogeneous 3D rat ventricle computational models, with architecture obtained from diffusion tensor MRI (DT-MRI) at a resolution of 200 µm and kinetics from the modified Pandit left and right ventricular cell models [14], to determine the relative roles of anisotropy (fibers) and orthotropy (sheets) on propagation. Details of using DT-MRI data in electrophysiological simulations, and integration methods for the models, are described in detail in [5]. Briefly, propagation in the ventricles is described by the non-linear cable equation:

$$\partial V/\partial t = \nabla(\mathrm{D}\nabla V) - I_{\mathrm{ion}}, \qquad (1)$$

where V is membrane potential, t is time, ∇ is a spatial gradient operator, D is the electrical diffusion tensor that characterizes electrotonic spread of voltage through the tissue and I_{ion} is the total membrane ionic current density. For I_{ion} we use the Pandit cell model that provides

formulations for left ventricular endocardial and epicardial cells (we apply a smooth parameter gradient across the left ventricular free wall and septum) as well as right ventricular cells. The eigenvectors obtained from DT-MRI are used to construct D at each node throughout the geometry (and therefore to reconstruct the fiber and sheet architecture of the myocardium) using:

$$\mathbf{D} = D_f \mathbf{f}\mathbf{f}^T + D_s \mathbf{s}\mathbf{s}^T + D_n \mathbf{n}\mathbf{n}^T \qquad (2)$$

where **f**, **s** and **n** are the primary, secondary and tertiary DT-MRI eigenvectors respectively (which correspond to the fiber, sheet and sheet normal directions respectively), D_f, D_s and D_n are the electrical diffusion coefficients in the three directions f, s and n, and the superscript T denotes vector transpose. For isotropic propagation we set the diffusion coefficients in the three directions to the same values, such that $D_f = D_s = D_n$ To introduce fiber anisotropy we set the ratio D_f: D_s = 4:1 and $D_s = D_n$ so that conduction velocity (CV) is twice as fast along the myofibre as across it. To introduce orthotropic propagation, the diffusion coefficients were set with the ratio D_f: D_s: D_n = 16:4:1 after [2] to give a CV ratio of 4:2:1 in the three directions **f**, **s** and **n** respectively. Three-dimensional activation and repolarization was simulated for each of the four pacing sites in virtual ventricles with: (i) isotropic conduction; (ii) anisotropic conduction; and in (iii) orthotropic ventricles. In each case simulations were carried out in the ventricles with the apex removed (as in the experiment) and with the apex present, so that the influence of the boundary of the cut transmural surface could be explored.

D. Measurement of Conduction Velocity

Data were analyzed using a customized software program written using PV-Wave software (Visual Numerics, Houstn, Tx). The local CV was measured as described in [11]. Briefly, the distributions of activation times for spatial regions of 5 x 5 pixels were fitted with a plane, and gradients of activation times gx and gy were calculated for each plane along the x and y axes, respectively. The magnitude of the local CV was calculated for each pixel as $(gx^2+gy^2)^{1/2}$. Transmural conduction velocity is obtained as the conduction velocity defined above in regions along the radial path from the stimulation point towards the centroid of the LV cavity, and circumferential conduction velocity from regions in the circumferential direction around the ventricular cavity.

III. Results

A. Myocardial Structure

Cut surface optical microscope images enabled the identification of the zones of the Tta and Cta and the TCI, and for the identification of the precise electrode position for each heart (Fig 1.). The identified Tta and Cta zones were later used for comparison of conduction velocity and activation contours. The identified location of the TCI was confirmed on high-resolution contrast enhanced MRI images (not shown, method as in [13]). The DT-MRI images obtained after optical activity mapping (and used as a geometry in the simulation model) were consistent with rat cardiac DT-MRI studies previously described [15].

B. Comparison of activation between experiment and simulation

The fine detail of activation patterns were compared between experiment and simulation in activation contour maps with 0.3 ms isochrones (Fig. 2.). A generally observed feature of experimental transmural wave propagation from the stimulation site is widely spaced isochrones in the Cta with tightly spaced isochrones in the Tta. This pattern is also observed (except immediately adjacent to the papillary muscles) in experimental normal sinus rhythm (data not shown) where activation is primarily from endocardium to epicardium, and tightly spaced contours are similarly observed in the Tta and widely spaced contours in the Cta. The same pattern of fast Cta conduction and slower Tta conduction is observed for experimental circumferential wave front conduction (Fig. 2). Comparison with the simulations in different myocardial architectural models allows the possible mechanisms for the differential propagation to be explored. In the isotropic virtual myocardium activation contours in the Cta and Tta are evenly spaced (as shown for posterior and lateral LV stimulation in Fig. 2, but also observed for septal and anterior LV stimulation). In the anistropic virtual myocardium the experimental findings are replicated, with slower radial and circumferential conduction in the Tta than Cta. In the orthotropic virtual ventricles the experimental findings are again replicated, with more pronounced differences between the Cta and Tta.

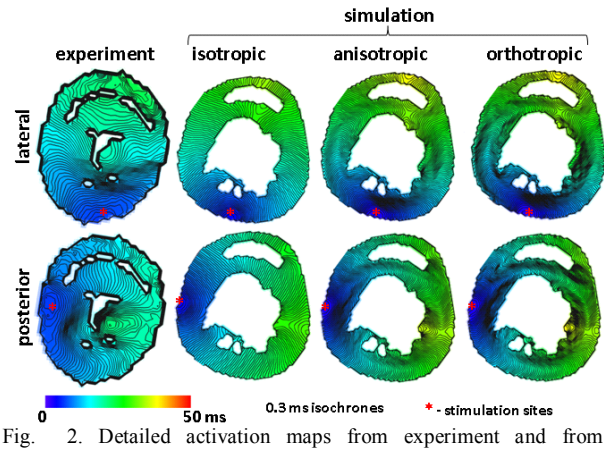

Fig. 2. Detailed activation maps from experiment and from simulations showing widely spaced contours in the compacta, with tightly packed contours in the trabeculata for both transverse conduction and circumferential propagation of the wave front from the stimulation electrode, for posterior and lateral sub-epicardial stimulation sites. The same pattern was observed in all other hearts (n = 4) for all LV stimulation sites.

In order to quantify the experimental differences between the rate of propagation in the Cta and Tta, and to better relate these to the model conditions quantitative conduction

velocity maps were generated. Conduction velocity for an example experimental heart and the virtual myocardial models are shown for posterior and lateral sub-epicardial stimulation in Fig. 3. Slower conduction in the Tta than the Cta is seen under all conditions, but is pronounced only in the experimental data and the orthotropic virtual myocardium. In the experimental study radial propagation is fast in the Cta: 69.4±40.3 and slow in the Tta: 31.9±15.0* (mean ± s.d cm·s-1, * $p < 0.01$ by two sample t-test). Circumferential propagation around the LV cavity is fast in the Cta: 63.2±19.5 and is slower in the Tta: 32.7±11.0*. In the simulations the pattern and velocity are not replicated in an isotropic model (**I**), are partially replicated in a simulation study including fiber anisotropy (**A**) and are more fully replicated in orthotropic (**O**) ventricles (fiber and sheet anisotropy). The radial propagation velocity is **I**: Cta: 74.6±26.8; Tta: 54.8±26.2*; **A**: Cta: 93.9±66.2; Tta: 36.6±12.8* **O**: Cta: 64.6±41.8; Tta: 40.4±13.19*. Circumferential velocity is, **I**: Cta: 54.2±3.9; Tta:54.3±3.9; **A**: Cta:43.6±3.2; Tta: 40.6±6.6; **O**: Cta: 63.2±19.5; Tta: 32.7±11.9*. Normal sinus activation was simulated in the isotropic, anisotropic and orthotropic virtual ventricles. The overall pattern of experimental activation was replicated in all the virtual myocardial except that in the experiment Cta conduction was faster than Tta conduction, whilst in the simulations Cta conduction and Tta conduction were similar. Also, the experimental early break though of activation in the RV was also not observed in the simulations (data not shown). This is in line with expected findings as the Purkinje system is not modeled.

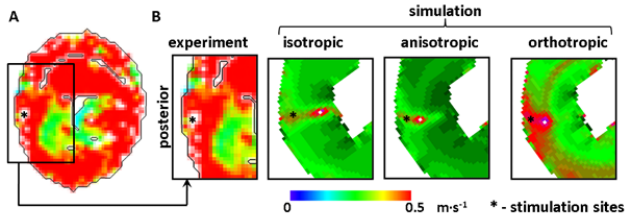

Fig. 3. Detailed conduction velocity maps from experiment and from simulations showing fast conduction in the compacta and slower conduction in the trabeculata for both radial conduction and circumferential conduction.

IV. DISCUSSION

The aim for this study was to further investigate the finding that the myocardial laminae influence electrical propagation [2] by exploring this phenomenon in a large region of the myocardium using optical mapping, rather than a relatively smaller region of the myocardium using plunge electrodes (as in [2]). The limitation of optical mapping to 2D imaging is overcome by a parallel experiment specific modeling. The rationale for recording activity on the cut myocardial surface is that myolaminae and myolaminar cleavage planes are largely absent in the superficial sub-epicardium, and access to the endocardium in structurally intact small mammalian hearts is technically challenging. Our experimental studies show that the propagating wave shows some consistent features irrespective of the chosen stimulation site (posterior LV, lateral LV, anterior LV, and septum). The radial and circumferential propagation of the wave front, close to the point of origin, are faster in the Cta and slower in the Tta, and furthermore, the same pattern of propagation is seen (slow Tta, fast Cta) from normal sinus activation, which largely initiates in the sub-endocardium. Possible reasons for this pattern of activation are: (i) fiber orientation effects, both the normal radial change, and the shift of the rate of change at the TCI; (ii) abrupt change in laminar orientation at the TCI [6] and the more complex orientation changes of the laminae in the Tta; (iii) the looser structure of the Tta with respect to the Cta; (iv) effects associated with possible gap junction/connexin distribution differences between the sub-epicardium and sub-endocardium; (v) effects associated with differing Purkinje network between the sub-epicardium and sub-endocardium.

Comparison of the experimental data with experiment specific computational simulations demonstrated that the observed experimental findings (fast Cta conduction, slow Tta conduction) are only partially replicated in isotropic virtual ventricles: there is a faster Cta and slower radial conduction but the rate of circumferential conduction is the same in the Cta and Tta. The different rate of Cta and Tta radial conduction may be associated with electrophysiological heterogeneity between rat LV sub-endocardial and sub-epicardial myocytes, which was incorporated into all the virtual myocardium models. The experimental findings of fast Cta and slow Cta radial and circumferential conduction are replicated in both the anisotropic and the orthotropic ventricles, but with a closer qualitative and quantitative match between the spatial and temporal pattern of activation to the orthotropic model than to the anisotropic model. Neither the anistropic model nor the orthotropic model incorporated the looser structure of the Tta with respect to the Cta, or Purkinje fiber differences between the Tta and Cta, or gap junction distribution differences between the Tta and Cta [16]. An implication of this is that the observed experimental activation pattern can be explained when only considering structural anisotropy/orthotropy. These preliminary findings are in agreement with [8], that more complex models incorporating structural differences between the Cta and Tta are required to reproduce experimentally recorded activation maps. The findings in this study are compatible with the description of laminar conduction described by [2] in that the model incorporating laminar conduction best reproduced the experimental findings.

There are some inherent limitations in the approach – both in recording and in simulating transmural activation. It is possible that the activation patterns recorded on the cut transmural surface will not be completely representative of activation patterns in the intact heart. A future direction will be to carry out the simulations using a bidomain diffusion model, instead of the monodomain diffusion model, as this

will simulate the bath loading effects at the cut surface. It is noted that the activation patterns and conduction velocities recorded and simulated are similar using the monodomain approach. A higher spatial-resolution computational geometry will be used in follow up studies to minimize effects of grid discretisation on calculated conduction velocity. In this study, the cardiac MRI images used for the computational model was not from one of the hearts which underwent optical mapping – a future direction will be to use the same geometry for experiments and simulations. An additional future direction will be to apply the experimental and simulation approach in hearts from disease models.

REFERENCES

[1] J. Jalife, "Ventricular fibrillation: mechanisms of initiation and maintenance," *Ann. Rev. Physiol*, vol. 62, pp. 25-50, 2000.

[2] D. A.Hooks, M. L. Trew, B. J. Caldwell, G. B. Sands, I. J. LeGrice and B. H. Smaill, "Laminar arrangement of ventricular myocytes influences electrical behavior of the heart," *Circ. Res.*, vol. 101(10):pp. e103-112., 2007.

[3] R.H. Clayton, E.A. Zhuchkova, A.V. Panfilov,"Phase singularities and filaments: simplifying complexity in computational models of ventricular fibrillation," *Prog. Biophys. Mol. Biol,* vol. 90, pp. 378-398, 2006.

[4] O. Bernus, M. Wellner, S. F. Mironov, A. M. Pertsov, "Simulation of vol.tage sensitive optical signals in three-dimensional slabs of cardiac tissue: application to transillumination and coaxial imaging methods," *Phys. Med. Biol.* Vol. 50, pp. 215-229, 2005.

[5] A. P. Benson, O. V. Aslanidi, H. Zhang, A. V. Holden, "The canine virtual ventricular wall: A platform for dissecting pharmacological effects on propagation and arrhythmogenesis" *Prog. Biophys. Mol. Biol,* vol. 96, pp. 187-208, 2008.

[6] D. D. Streeter, "Gross Morphology and fibre geometry of the Heart" in *Handbook of Physiology, V*ol. 1 . *The Heart*, R. M. Berne, N. Sperelakis, and S. R. Geigert Ed. Bethesda, MD: American Physiological Society, 1979, pp. 61-112.

[7] D. K. Dawson, A. M. Maceira, V. J. Raj, C. Graham, D. J. Pennell, P. J. Kilner, "Regional Thicknesses and Thickening of Compacted and Trabeculated Myocardial Layers of the Normal Left Ventricle Studied by Cardiovascular Magnetic Resonance," *Circ. Cardiovasc. Imaging,* vol. 4(2) pp. 139-146, 2011.

[8] R. Hren, J. Nenonen,B. M. Horácek, "Simulated epicardial potential maps during paced activation reflect myocardial fibrous structure," *Ann. Biomed. Eng.,* vol. 26(6), pp. 1022-1035, Nov 1998.

[9] B. Taccardi,E. Macchi, R. L. Lux, P. R. Ershler, S. Spaggiari, S. Baruffi, and Y. Vyhmeister. "Effect of myocardial fiber direction on epicardial potentials," *Circulation* vol. 90, pp. 3076-3090, 1994.

[10] V. V. Fedorov, I. T. Lozinsky, E. A. Sosunov, E. P. Anyukhovsky, M. R. Rosen, C. W. Balke, I. R. Efimov "Application of blebbistatin as an excitation-contraction uncoupler for electrophysiologic study of rat and rabbit hearts," *Heart Rhythm*, vol. 4(5), pp. 619-626, 2007.

[11] P. V. Bayly, B. H. KenKnight, J. M. Rogers,R. E. Hillsley, R. E. Ideker, W. M. Smith, "Estimation of conduction velocity vector fields from epicardial mapping data," *IEEE Trans. Biomed. Eng.,* vol. 45, pp. 563-571, 1998.

[12] R.D. Walton, D. Benoist, C. J. Hyatt, S. H. Gilbert, E. White, O. Bernus, "Dual excitation wavelength epifluorescence imaging of transmural electrophysiological properties in intact hearts," *Heart Rhythm*, vol. 7(12), pp. 1843-1849, 2010.

[13] A. P. Benson, O. Bernus, H. Dierckx, S. H. Gilbert, J. P. Greenwood, A. V. Holden et. al., "Construction and validation of anisotropic and orthotropic ventricular geometries for quantitative predictive cardiac electrophysiology" Interface Focus vol. 6, pp. 101-116, 2011.

[14] S. F. Noujaim, S. V. Pandit, O. Berenfeld, K. Vikstrom, M. Cerrone, S. Mironov, et. al., " Up-regulation of the inward rectifier K+ current (I K1) in the mouse heart accelerates and stabilizes rotors," *J. Physiol.,* vol. *578, pp.* 315-326, 2007.

[15] S. H. Gilbert, A. P. Benson, P. Li, A. V. Holden. "Regional localisation of left ventricular sheet structure: integration with current models of cardiac fibre, sheet and band structure," Eur. *Jour. Cardiothorac Surg.*, vol. 32(2), pp. 231-249, 2007.

[16] K. A. Yamada, E. M. Kanter, K. G. Green, J. E. Saffitz, "Transmural distribution of connexins in rodent hearts,". *J. Cardiovasc. Electrophysiol.*, vol. 15(6), pp. 710-715, 2004.